

Research Article

Yingchun Cao, Nancy P. Sanchez, Wenzhe Jiang, Wei Ren, Rafał Lewicki, Dongfang Jiang, Robert J. Griffin and Frank K. Tittel*

Multi-pass absorption spectroscopy for H₂O₂ detection using a CW DFB-QCL

Abstract: Hydrogen peroxide (H₂O₂) detection was demonstrated with multi-pass absorption spectroscopy using a commercial 76-m astigmatic multi-pass absorption cell. An ~773- μ m continuous wave, distributed feedback quantum cascade laser (CW DFB-QCL) was employed for targeting a strong H₂O₂ line (1296.2 cm⁻¹) in the fundamental absorption band. Wavelength modulation spectroscopy combined with a second harmonic detection technique was utilized to increase the signal-to-noise ratio. By optimizing the pressure inside the multi-pass cell and the wavelength modulation depth, a minimum detection limit (1 σ) of 13.4 ppbv was achieved for H₂O₂ with a 2-s sampling time. From an Allan-Werle deviation plot, the detection limit could be improved to 1.5 ppbv with an averaging time of 200 s. Interference effects of atmospheric air components are also discussed.

Keywords: hydrogen peroxide; laser spectroscopy; mid-infrared; multi-pass absorption cell; quantum cascade lasers; wavelength modulation spectroscopy.

OCIS codes: (280.3420) Laser sensors; (300.6340) Spectroscopy, infrared; (140.5965) Semiconductor lasers, quantum cascade; (120.4640) Optical instruments.

DOI 10.1515/aot-2014-0052

Received October 13, 2014; accepted November 4, 2014

***Corresponding author: Frank K. Tittel**, Electrical and Computer Engineering Department, Rice University, 6100 Main St. Houston, TX 77005, USA, e-mail: fkt@rice.edu

Yingchun Cao, Wenzhe Jiang, Rafał Lewicki and Dongfang Jiang: Electrical and Computer Engineering Department, Rice University, 6100 Main St. Houston, TX 77005, USA

Nancy P. Sanchez and Robert J. Griffin: Civil and Environmental Engineering Department, Rice University, 6100 Main St. Houston, TX 77005, USA

Wei Ren: Mechanical and Automation Engineering Department, Chinese University of Hong Kong, New Territories, Hong Kong

www.degruyter.com/aot

© 2014 THOSS Media and De Gruyter

1 Introduction

Hydrogen peroxide (H₂O₂) is an important atmospheric trace gas that is formed mainly by combination of hydroperoxyl radicals [1]. H₂O₂ acts as a reservoir for HO_x radicals (e.g., OH and HO₂) and, therefore, plays an important role in the oxidative capacity of the atmosphere. Furthermore, H₂O₂ participates in the formation of sulfate aerosol by in-cloud oxidation of S(IV) to S(VI), which is closely linked with the phenomena of acid fog and rain [2–4]. Owing to its high reactivity and low concentration (ppbv to sub-ppbv levels [5–7]), the detection of atmospheric H₂O₂ involves specific challenges.

Traditional approaches for determination of H₂O₂ in the atmosphere are often based on wet chemistry techniques, in which transfer of H₂O₂ from the gas phase to the liquid phase is required for subsequent determination by techniques such as fluorescence spectroscopy [8, 9]. Sampling artifacts and interferences from other atmospheric constituents may be introduced in these methods and can cause an additional error in the H₂O₂ concentration determination. Therefore, direct concentration measurements of gas-phase H₂O₂ offers significant practical advantages.

Tunable diode laser absorption spectroscopy (TDLAS) is a widely used tool for gas detection due to its high sensitivity and selectivity. Gas-phase H₂O₂ detection based on TDLAS has been reported by several research groups. Slemr et al. demonstrated gas-phase H₂O₂ measurement by using a 40-m multi-pass White cell and reported a detection limit of 2.9 ppbv with a 5-min averaging time [10]. Lindley et al. utilized a quantum cascade laser (QCL)-based TDLAS technology using a 100.1-m astigmatic multi-pass cell (MPC) and obtained a H₂O₂ detection limit of 15 and 3 ppbv for walkthrough portal and optical bench top instruments, respectively [11]. However, the large number of co-added spectra complicates data processing and increases the data acquisition time. Another TDLAS system with a H₂O₂ detection limit of 110 pptv for a 1-s averaging time was demonstrated by McManus et al. [12]. Their low detection

limit was obtained using a long path-length gas absorption cell (260 m with 554 passes). More recently, H₂O₂ detection based on a sensitive quartz-enhanced photoacoustic spectroscopy technique with a continuous wave (CW), distributed feedback (DFB) QCL was reported by our group. With this H₂O₂ sensor, detection limits of 75 ppbv for a 1-s sampling time and of 12 ppbv for 100-s averaging time were achieved [13]. Other spectroscopic methods such as cavity-enhanced optical frequency comb spectroscopy have been demonstrated for gas-phase H₂O₂ detection with a detection limit of 130 ppb in the presence of 2.8% water [14].

In this paper, a TDLAS-based sensor system capable of sensitive, selective gas-phase H₂O₂ detection and using a CW DFB QCL targeting a strong H₂O₂ absorption line at $\sim 1296.2\text{ cm}^{-1}$ was demonstrated.

2 Experimental configuration

The H₂O₂ sensor system is depicted in Figure 1. A thermoelectrically cooled (TEC) CW DFB-QCL (Corning Inc., New York, USA) operating at 7.73 μm was used as the excitation laser source. The laser wavelength was tuned with a temperature controller (TED 200C, Thorlabs, Inc., Newton, NJ, USA) to coincide with the targeted H₂O₂ absorption line. In addition, a low-frequency sawtooth wave and a high-frequency sinusoidal wave provided by a

function generator (AFG 3102, Tektronix, Inc., Beaverton, OR, USA) were combined and sent to a current controller (LDX 3232, ILX Lightwave, Bozeman, MT, USA) to realize QCL wavelength scanning and modulation across the H₂O₂ absorption line, respectively.

The CW-DFB-QCL beam was directed to a wedged beam splitter (Thorlabs, Inc., Newton, NJ, USA) and focused by three plano-convex lenses (Thorlabs, Inc., Newton, NJ, USA), L₁ (f=50 mm), L₂ (f=100 mm), and L₃ (f=250 mm), at the center of a commercial multi-pass gas absorption cell (AMAC-76, Aerodyne Research, Inc., Billerica, MA, USA). A pinhole (D=400 μm) (Thorlabs, Inc., Newton, NJ, USA) was employed between L₁ and L₂ to further improve the beam shape and meet the optical requirement of the MPC. The QCL beam exiting from the MPC was collected by a parabolic mirror (Thorlabs, Inc., Newton, NJ, USA) and directed to a mid-infrared detector (PVM1-3TE-8, Vigo System S.A., Ożarów Mazowiecki, Poland). The electric signal from this detector was demodulated by a lock-in amplifier (Model 7265, Signal Recovery, Oak Ridge, TN, USA) and acquired with a data acquisition (DAQ) card (DAQCard-AI-16XE-50, National Instruments, Austin, TX, USA). The two reflected beams from the beam splitter were utilized for wavelength locking and power normalization, respectively. One of the reflected beams is passed through a reference gas cell (Thorlabs, Inc., Newton, NJ, USA) containing 1% N₂O at a pressure of 150 Torr and was detected by a pyroelectric detector (LIE-332f, InfraTec,

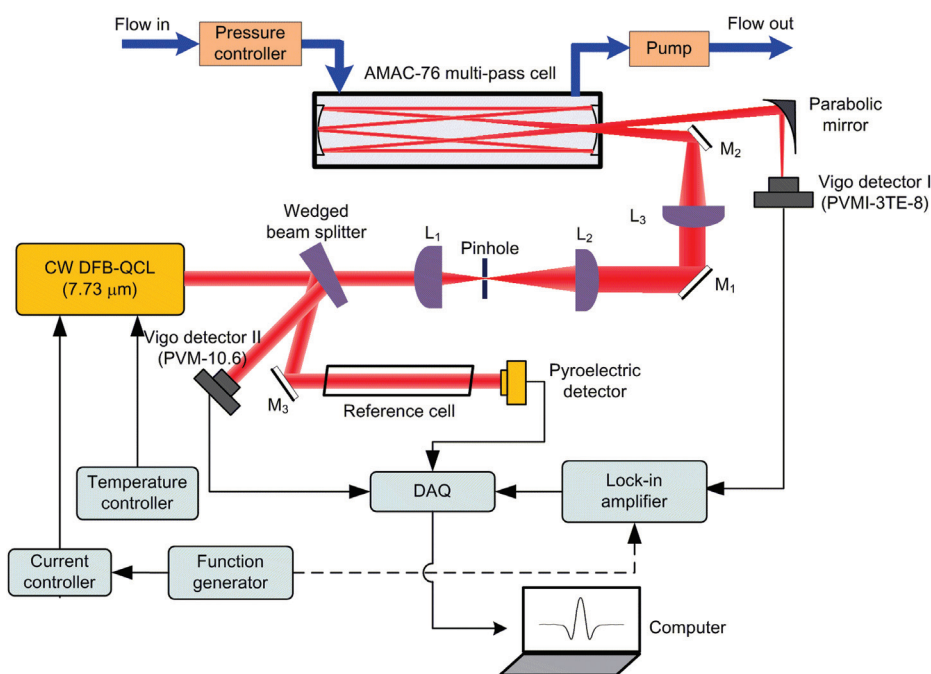


Figure 1 Schematic of the H₂O₂ sensor system. L, lens; M, mirror; DAQ, data acquisition.

Dresden, Germany) to reduce the noise associated with QCL wavelength drifts. The QCL wavelength was locked to a N_2O absorption line at 1296.27 cm^{-1} in order to target the adjacent optimum H_2O_2 absorption line (1296.2 cm^{-1}). The reflected beam also was detected by a second IR detector (PVM-10.6, Vigo System S.A., Ożarów Mazowiecki, Poland) to monitor the presence of potential QCL power variations. The H_2O_2 gas flow entering the MPC was controlled using a pressure controller (#649, MKS Instruments, Inc., Andover, MA, USA) and an oil-free vacuum pump (#813.5, KNF, Freiburg, Germany).

3 System optimization and selection of the target H_2O_2 absorption line

3.1 Laser beam optimization

A critical step in the design of a MPC-based gas sensor system is to optimize the coupling of the QCL beam into the gas cell with minimum optical noise introduced due to scattered light at the entrance and exit MPC holes and beam interference inside the MPC. The MPC used in our system is an Aerodyne, Inc. AMAC-76 astigmatic Herriott cell with a volume of 0.5 l and mechanical length of 32 cm [15]. The laser beam was focused at the center of the MPC, with a working distance larger than half of the cell length. In our H_2O_2 sensor system, three plano-convex lenses were used to reshape the laser beam and focus the beam efficiently into the MPC as mentioned in Section 2. The

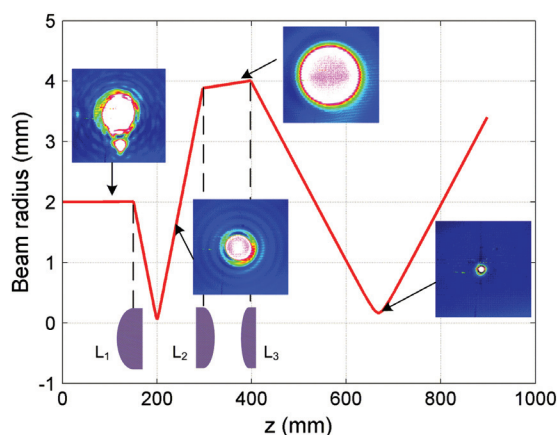


Figure 2 Laser beam radius evolution resulting from the use of three plano-convex lenses, L_1 ($f=50\text{ mm}$), L_2 ($f=100\text{ mm}$), and L_3 ($f=250\text{ mm}$). The red curve is the theoretical beam radius variation along the propagation direction, the inset beam patterns were measured by an IR camera, and the dashed line indicates the positions of the three lenses.

QCL beam size was calculated by means of the Gaussian beam equation [16] along the propagation direction and shown (red curve) in Figure 2. The separation distances are 148 mm between L_1 and L_2 and 100 mm between L_2 and L_3 . The focusing point at the center of the MPC is 270 mm from L_3 , with a beam waist $<1\text{ mm}$. The experimental beam evolution was recorded using an IR camera (PV320, Electro-Physics Corp., Fairfield, NJ, USA) at several positions and shown in Figure 2. The beam sizes at these positions agree well with the theoretical design. To eliminate the imperfect pattern of the initial laser beam (inset in Figure 2 prior to L_1), a pinhole with a diameter of $400\text{ }\mu\text{m}$ is inserted at the focal point of lens L_1 as a spatial filter. A QCL beam with circular shape was obtained at the focal point of lens L_3 .

3.2 MPC optical path-length verification

A visible red laser beam co-aligned with the QCL beam was injected after the wedged beam splitter to facilitate the alignment of the mid-infrared QCL beam through the MPC. After adjusting the entrance angle of the incoming red laser beam, the correct beam pattern, resulting in 238 passes between the MPC mirrors, was obtained for the MPC and shown as an inset in Figure 3. An effective path-length of 76 m was obtained with this alignment. To verify this MPC path length, a cylinder containing 5.4 ppm methane (CH_4) was used to measure the absorption in the MPC at $\sim 1297.5\text{ cm}^{-1}$ and at a pressure of 100 Torr . The effective absorption length agreed with the expected optical path length within $\pm 1\%$ by comparing the CH_4 transmission peaks with the HITRAN database [17].

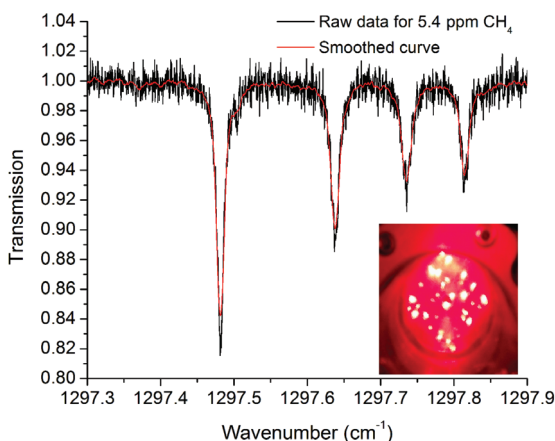


Figure 3 Experimentally measured transmission curve of 5.4 ppm CH_4 with the MPC used in our system at 100 Torr . The inset figure shows the trace laser beam pattern observed on the front mirror of the MPC.

3.3 H₂O₂ line selection and optimization

H₂O₂ absorption lines in the ν_6 fundamental ro-vibrational band in the 7.4–8.4 μm spectral range were considered to be optimum due to their strong absorption. Figure 4A depicts a HITRAN-based absorption spectrum [17] simulated for 1 ppm gas-phase H₂O₂ (red line) balanced by pure N₂ at 296 K and 30 Torr within a 1295.95–1296.3 cm⁻¹ spectral range. The absorption spectrum of air is also presented in Figure 4A for comparison. It is found that there are two groups of strong H₂O₂ absorption lines, labeled as single peak (1296.01 cm⁻¹) and double peak (1296.2 cm⁻¹) in this spectral region that show a small overlap with interference from absorption peaks in air. These two groups of peaks were selected as suitable H₂O₂ lines for further measurements. Experimental second harmonic (2*f*) signals of H₂O₂, air, and pure N₂ were recorded using wavelength modulation spectroscopy with the second harmonic (2*f*-WMS) detection method, as shown in Figure 4B. The strong single peak and double peak of H₂O₂ could be easily distinguished from the curve with very low interferences from air constituents.

In order to achieve a better system detection sensitivity, the pressure inside the MPC and the modulation depth for WMS should be optimized [18, 19]. Gas-phase H₂O₂ with a fixed concentration was generated by mixing an air flow with H₂O₂ vapor generated by a closed container filled with a 10% H₂O₂ solution. For each individual pressure ranging from 30 Torr to 250 Torr, the 2*f* signals for both single peak

(open circles) and double peak (solid dots) were recorded with a 5-kHz modulation frequency and different modulation depths as shown in Figure 5A. According to Figure 5A, the maximum signal for the single peak is achieved for a 5-mA modulation depth at 150 Torr, while that for the double peak is obtained for a modulation depth of 8 mA at 150 Torr. To better understand this behavior, the entire 2*f* signal curves are plotted in Figure 5B and 5C for several pressure and modulation depth combinations. It was found that at low pressures (<100 Torr), the H₂O₂ peaks are broadened with increasing pressure and modulation depth, and the peak amplitude value for the single peak is slightly higher than that of the double peak for each individual operation combination. However, when the pressure is increased, the double peak becomes a single wide peak due to the line-broadening effect, which results in a large increase for the peak amplitude value. From these data, the optimal operation conditions for the H₂O₂ sensor system were determined to be an 8-mA modulation depth and a 150-Torr pressure.

4 System performance and discussion

A 2*f*-WMS method was utilized to carry out the H₂O₂ concentration measurements. The wavelength of the QCL was tuned to the double peak of H₂O₂ at ~1296.2 cm⁻¹ (240 mÅ,

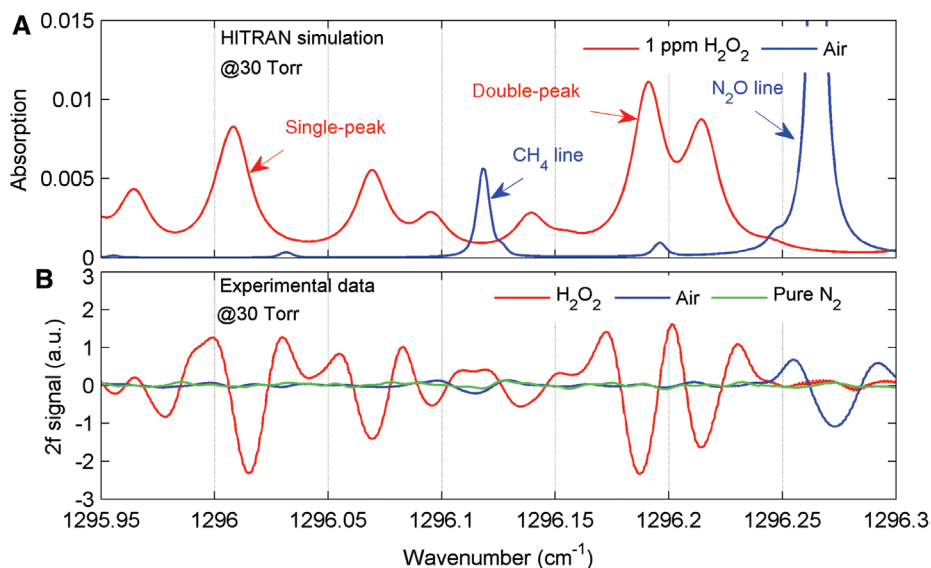


Figure 4 H₂O₂ absorption spectra and air at a pressure of 30 Torr. (A) CH₄ and N₂O absorption results from the HITRAN database; (B) 2*f* signals from experimental measurements. Single-peak and double-peak represent two groups of strong H₂O₂ absorption lines at ~1296.01 cm⁻¹ and ~1296.2 cm⁻¹, respectively.

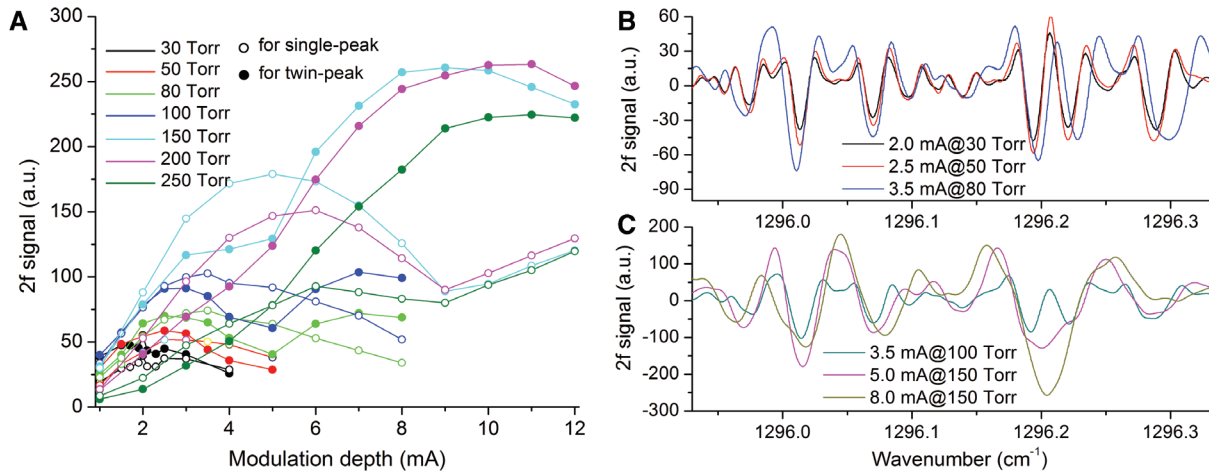


Figure 5 (A) Peak values of $2f$ signals at single peak (open circles) and double peak (solid dots) for different pressures and modulation depths; (B) $2f$ signal curves for different operating conditions at lower pressures; (C) $2f$ signal curves for different operating conditions at higher pressures.

27°C). Two current signals, with sawtooth (10 mA, 0.5 Hz) and sinusoidal (8 mA, 5 kHz) waves, were combined and sent to the current controller to realize both laser wavelength scanning and modulation at the same time. The DC part of the main detector output was recorded to show the transmission of the MPC, while the AC part was delivered to the lock-in amplifier for $2f$ signal demodulation. The pressure inside the MPC was controlled at 150 Torr for maximum signal generation.

4.1 Sensitivity calibration

The sensitivity calibration of the sensing system was carried out by mixing the air flow with the H_2O_2 vapor

produced by a 30% H_2O_2 solution (w/w). As it takes several minutes for the H_2O_2 concentration to reach a constant level in the MPC, several groups of data for both the transmissions and the $2f$ signals were recorded at constant time intervals during the period of concentration stabilization. The H_2O_2 concentrations are calibrated by fitting the transmission curves to the standard HITRAN transmission values with the same operating conditions [17]. A lock-in amplifier time constant of 50 ms was selected for optimal $2f$ signal demodulation within the 2-s ramp period. The $2f$ signal curves across the target H_2O_2 line for H_2O_2 concentrations from 0.5 ppm to 10 ppm are plotted in Figure 6A. The peak values for different H_2O_2 concentration signals are plotted in Figure 6B. The fit shows linear relationship with a R^2 value >0.999 and a proportionality coefficient of

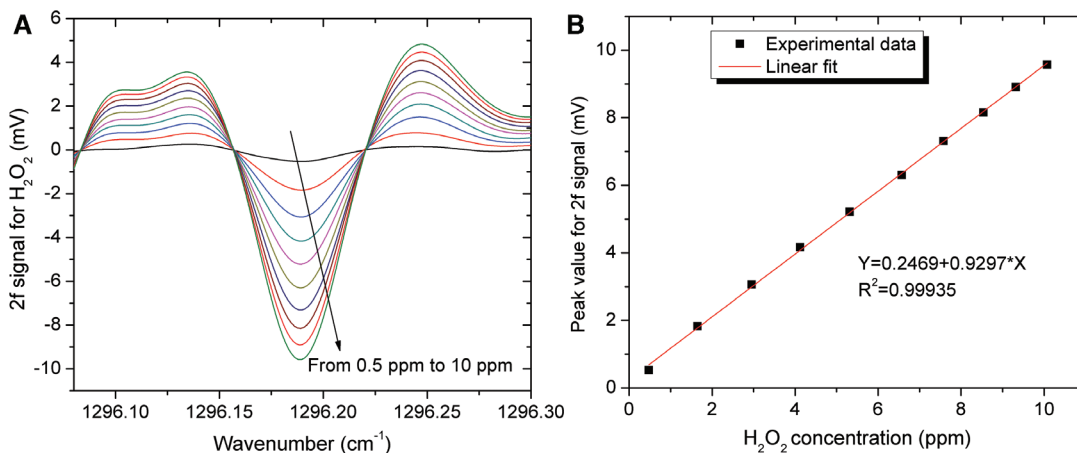


Figure 6 Calibration for the H_2O_2 detection system. (A) $2f$ signals for different H_2O_2 concentrations as the laser wavelength is scanned across the double peak; (B) peak $2f$ signals vs. H_2O_2 concentration values.

$k=0.9297$ mV/ppm. The intercept of 0.2469 mV originates from the baseline.

4.2 Noise level analysis

The noise level analysis of our system was accomplished based on the Allan-Werle variance [20]. To avoid the noise induced by absorption change, we used pure N₂ as the detection gas. The $2f$ magnitude in terms of H₂O₂ concentration at the double-peak position was monitored for ~3 h, as shown in Figure 7A. An Allan-Werle deviation analysis is employed for investigating the long-term stability and precision of the H₂O₂ measurements for the reported H₂O₂ detection system, as shown in Figure 7B. A 1σ minimum detection limit (MDL) of 13.4 ppbv was achieved for H₂O₂ with our sensor system at a 2-s sampling time. If the averaging time is increased to an optimal value of 200 s, the MDL can be improved to 1.5 ppbv, as deduced from the Allan deviation plot.

These results were verified by evaluating the sensor system at low H₂O₂ concentration levels. A ppbv-level H₂O₂ concentration was generated by passing an air flow over 0.1% H₂O₂ solution (w/w) with a constant flow rate of 300 cm³/min. The H₂O₂ vapor concentration in the mixed gases was estimated to be ~30 ppb according to the sensitivity calibration described in Section 4.1. After a period of time, the H₂O₂ solution was consecutively exchanged with pure water. The $2f$ signals in terms of H₂O₂ concentration for these changes are plotted in Figure 8, where 30 ppb H₂O₂ corresponds to the environment of 0.1% H₂O₂ solution mixed with air flow, and zero air shows the pure

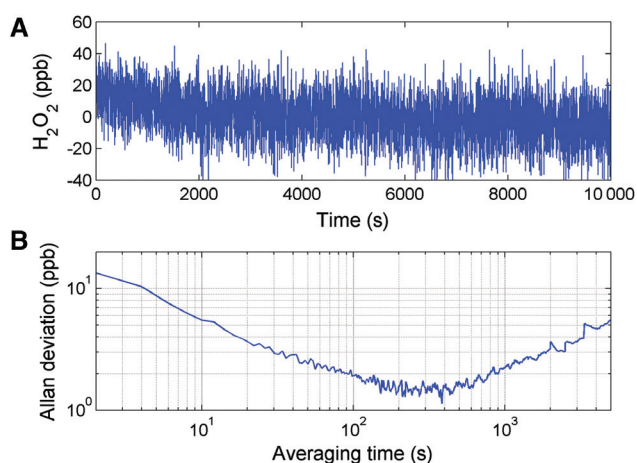


Figure 7 (A) Signal in terms of the H₂O₂ concentration with pure N₂; (B) Allan deviation in ppb for the signal in Figure 7A as a function of the averaging time.

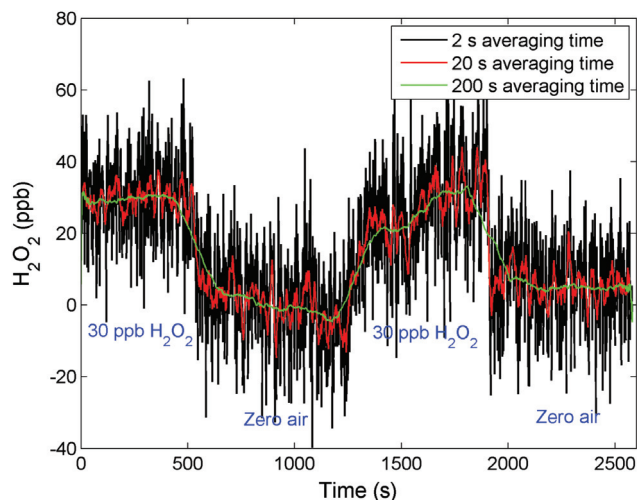


Figure 8 Low H₂O₂ concentration measurements. Lines with different colors show the measured signal behavior of our system at different averaging times.

water vapor mixed with air flow (background). This figure clearly shows the change in the measured H₂O₂ concentration levels when switching between the 30 ppb H₂O₂ and zero gas mixtures. With increased averaging time, as indicated by red and green lines in Figure 8, these changes become more evident, indicating that a lower detection limit can be obtained with a longer averaging time, as expected from Figure 7. The response time for a H₂O₂ concentration change for consecutive environment alternation is ~120 s. This long time response is due to the absorption/adsorption of H₂O₂ onto the MPC walls and gas lines. Appropriate treatments such as coating the glass surface of the MPC with a layer of special material in order to limit the adsorption effects [21], or heating the gas cell with a temperature-controllable thermal tape, can lead to a significant reduction in this response time.

4.3 Atmospheric H₂O₂ detection limit determined by gas interference

As discussed in Section 3.3, the double peak of H₂O₂ at ~1296.2 cm⁻¹ was selected as the target absorption feature due to its line strength and limited overlapping with other molecules present in the atmospheric air. In laboratory measurements, the concentrations of air components are relatively constant, and the prepared H₂O₂ concentration can generally ensure a large signal-to-noise ratio. In this case, there is no significant concern about a potential gas interference issue. However, for in-field atmospheric H₂O₂ measurements, the low concentration of H₂O₂ (~ppb to

sub-ppb in the atmosphere) and unpredictable variations in concentration of air components may introduce significant challenges for H_2O_2 environmental measurements. Therefore, the gas interference might be an important factor that limits the final system behavior and potential application in field campaigns.

For our system, where the pressure is controlled to 150 Torr, the line-broadening effect will enhance this interference. In order to show the interferences from other atmospheric gases that have absorption features within the laser tuning range, the absorption spectra of H_2O , N_2O , and CH_4 were simulated at 150 Torr using the HITRAN database and are plotted in Figure 9A. For comparison, the absorption lines for air and 1 ppm H_2O_2 also are depicted. It is shown that the interferences from air components are considerable for both the double peak and single peak. These absorption lines also are simulated at a lower pressure of

38 Torr as shown in Figure 9B. As expected, the interferences of air components become less significant due to decrease in line width. Table 1 presents the interferences of air components on selected H_2O_2 line positions at different pressures. These values represent the equivalent H_2O_2 concentrations with absorptions equal to that of a 10% concentration change for each air component. Table 1 shows that for a 150-Torr pressure, H_2O is the major interfering species, and the change in absorption for the double peak resulting from a 10% H_2O concentration change in air is equal to a concentration variation of ~ 43 ppb H_2O_2 . For the single peak, this value (~ 26.6 ppb) is also much greater than the atmospheric H_2O_2 concentration. However, as the pressure decreases to 38 Torr, these interference effects are reduced significantly, resulting in a total interference of 3.2 ppb for the single peak and 8 ppb for the double peak. However, in this case, the MDL of the system will

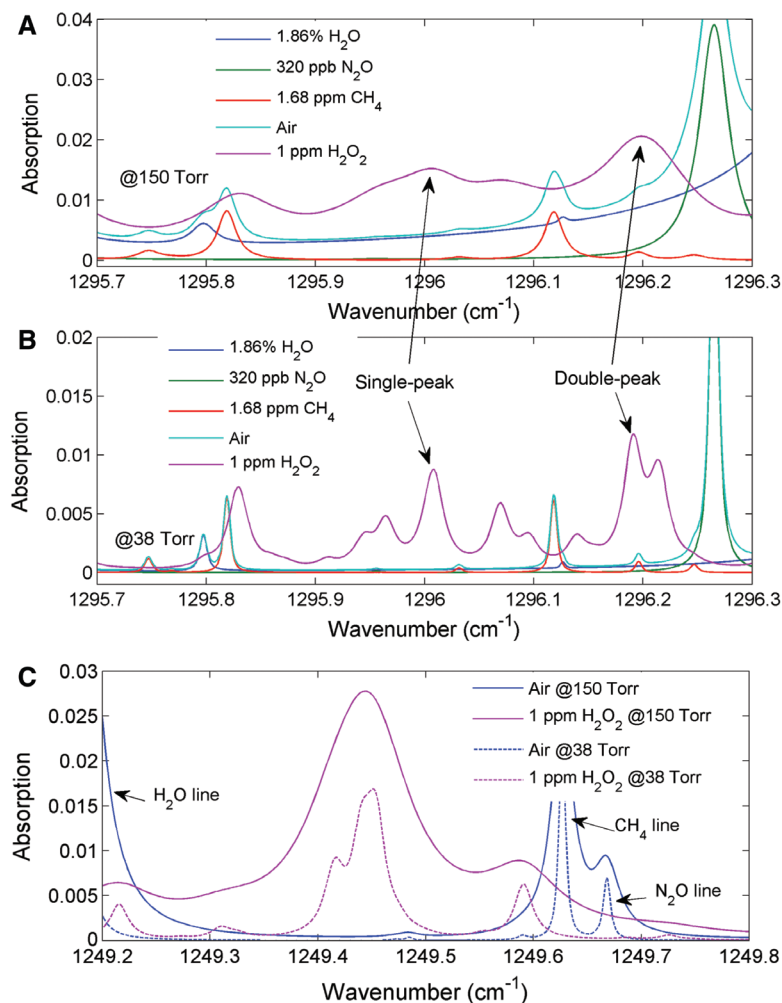


Figure 9 Interference effects of individual air components (H_2O , N_2O , CH_4 , and air) adjacent to H_2O_2 absorption lines acquired with a 76-m path length at pressures of (A) 150 Torr and (B) 38 Torr; (C) optimum H_2O_2 absorption line at ~ 1249.45 cm^{-1} compared with air absorption at 150 and 38 Torr for an absorption length of 76 m.

Table 1 Equivalent H₂O₂ concentrations in ppb due to a 10% concentration change of air components at single-peak absorption (1296.01 cm⁻¹), double-peak absorption (1296.2 cm⁻¹), and the optimum H₂O₂ absorption (1249.45 cm⁻¹) positions.

H ₂ O ₂ lines	P (Torr)	1.86% H ₂ O	320 ppb N ₂ O	1.68 ppm CH ₄
Single-peak line (1296.01 cm ⁻¹)	38	2.90	0.15	0.15
	75	9.57	0.52	0.51
	112	17.83	0.99	0.92
	150	26.58	1.49	1.29
Double-peak line (1296.2 cm ⁻¹)	38	4.53	0.99	2.50
	75	14.40	3.40	7.51
	112	27.40	6.82	6.69
	150	43.01	10.48	6.60
Optimum H ₂ O ₂ absorption line (1249.45 cm ⁻¹)	38	0.031	0.015	0.030
	75	0.131	0.058	0.121
	112	0.295	0.125	0.270
	150	0.523	0.221	0.500

become much larger due to the significant signal loss, as indicated in Figure 5, which will prevent the sensor from being able to quantify atmospheric H₂O₂ concentrations.

Based on the above discussion, the selected H₂O₂ absorption line at 1296.2 cm⁻¹ for our sensor system might not be able to realize accurate atmospheric H₂O₂ detection due to the limited sensitivity and interference from air components. By investigating all the H₂O₂ absorption lines in the mid-infrared spectral region, an optimum H₂O₂ line at 1249.45 cm⁻¹ appears as a better candidate for H₂O₂ detection due to its strong absorption and ultra-small interference from air constituents. The absorption curves of this optimum H₂O₂ line are presented in Figure 9C at pressures of 150 Torr and 38 Torr with a path length of 76 m. The interference from atmospheric air is negligible at the optimum H₂O₂ line position. The equivalent H₂O₂ concentration changes caused by a 10% air component concentration change are presented in Table 1 for comparison. The interferences from air result in ppt-level H₂O₂ concentration changes, which are much smaller than the atmospheric H₂O₂ concentration. Therefore, our sensor system targeting this optimum H₂O₂ line (1249.45 cm⁻¹) with an appropriate QCL wavelength could achieve atmospheric H₂O₂ detection overcoming potential interferences from air.

5 Conclusions

A H₂O₂ detection system based on multi-pass absorption spectroscopy was demonstrated. A 7.73- μ m CW DFB-QCL was used to target the strong H₂O₂ absorption line at 1296.2 cm⁻¹ in the ν_6 fundamental absorption band.

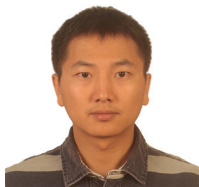
An astigmatic Herriott MPC with an effective optical path length of 76 m was employed to measure low H₂O₂ concentrations. Wavelength modulation spectroscopy with second harmonic detection was utilized to achieve optimum H₂O₂ detection sensitivity. A 1 σ MDL of 13.4 ppbv for H₂O₂ concentration measurement was achieved with an acquisition time of 2 s. This value could be improved to 1.5 ppbv after implementing an integration time of 200 s based on an Allan-Werle deviation analysis. Furthermore, observed interference effects due to atmospheric air components are discussed for different conditions to provide insight into potential limitations of using mid-infrared multi-pass absorption spectroscopy for atmospheric H₂O₂ detection. Finally, an optimum H₂O₂ absorption line at 1249.45 cm⁻¹ (~8 μ m) was suggested for even better performance of the sensor system.

Acknowledgments: The authors gratefully acknowledge the financial support from a National Science Foundation (NSF) ERC MIRTHE award, a NSF-ANR award for international collaboration in chemistry, “Next generation of Compact Infrared Laser based Sensor for Environmental Monitoring (NexCILAS),” and the Robert Welch Foundation grant C-0586.

References

- [1] W. R. Stockwell, *J. Geophys. Res.* 100(D6), 11695–11698 (1995).
- [2] B. J. Finlayson-Pitts and J. N. Pitts Jr., *Chemistry of the Upper and Lower Atmosphere-Theory, Experiments, and Applications*. (Academic, San Diego, 2000).
- [3] S. A. Penkett, B. J. Bandy, C. E. Reeves, D. McKenna and P. Hignett, *Faraday Discuss.* 100, 155–174 (1995).

- [4] D. Vione, V. Maurino, C. Minero and E. Pelizzetti, *Ann. Chim.* 93(4), 477–488 (2003).
- [5] R. Balasubramanian and L. Husain, *J. Geophys. Res.-Atmos.* 102(D17), 21209–21220 (1997).
- [6] V. P. Aneja and M. Das, *J. Appl. Meteorol.* 34, 1890–1898 (1995).
- [7] T. Yamashita, H. Sakugawa and K. Fujiwara, *Nippon Kagaku Kaishi* 12, 1127–1133 (1994).
- [8] H. Sakugawa, I. R. Kaplan, W. Tsai and Y. Cohen, *Environ. Sci. Technol.* 24(10), 1452–1462 (1990).
- [9] M. Lee, B. G. Heikes and D. W. O’Sullivan, *Atmos. Environ.* 34, 3475–3494 (2000).
- [10] F. Slemr, G. W. Harris, D. R. Hastie, G. I. Mackay and H. I. Schiff, *J. Geophys. Res. Atmos.* 91(D5), 5371–5378 (1986).
- [11] R. Lindley, E. Normand, M. McCulloch, P. Black, I. Howieson, et al., *Proc. SPIE* 7119, 71190K (2008).
- [12] J. B. McManus, M. S. Zahniser and D. D. Nelson, *Appl. Opt.* 50(4), A74–A85 (2011).
- [13] W. Ren, W. Jiang, N. P. Sanchez, P. Patimisco, V. Spagnolo, et al., *Appl. Phys. Lett.* 104, 041117 (2014).
- [14] A. Foltynowicz, P. Masłowski, A. J. Fleisher, B. J. Bjork and J. Ye, *Appl. Phys. B* 110, 163–175 (2013).
- [15] J. B. McManus, P. L. Keabian and M. S. Zahniser, *Appl. Opt.* 34(18), 3336–3348 (1995).
- [16] H. Kogelnik and T. Li, *Appl. Opt.* 5(10), 1550–1567 (1966).
- [17] L. S. Rothman, I. E. Gordon, A. Barbe, D. Chris Benner, P. F. Bernath, et al., *J. Quant. Spectrosc. Radiat. Transf.* 110(9–10), 533–572 (2009).
- [18] P. Werle, *Spectrochim. Acta A* 54(2), 197–236 (1998).
- [19] S. Schilt, L. Thévenaz and P. Robert, *Appl. Opt.* 42(33), 6728–6738 (2003).
- [20] P. Werle, R. Mücke and F. Slemr, *Appl. Phys. B* 57(2), 131–139 (1993).
- [21] J. B. McManus, J. H. Shorter, D. D. Nelson and M. S. Zahniser, *Sensors*, 2007 IEEE, 1341–1344 (2007).



Yingchun Cao

Electrical and Computer Engineering
Department, Rice University, 6100 Main St.
Houston, TX 77005, USA

Yingchun Cao received his BS and ME degree in Applied Physics and Physical Electronics from Huazhong University of Science and Technology (Wuhan, China) in 2007 and 2009, respectively, and a PhD degree in Electrical Engineering from The Hong Kong Polytechnic University (Hong Kong, China) in 2012. In February 2014, he joined the Laser Science Group at Rice University in Houston, TX, as a postdoctoral research associate. His current research interest is focused on the design and implementation of novel optical sensors based on mid-infrared lasers such as quantum cascade and interband cascade lasers for environmental applications.



Nancy P. Sanchez

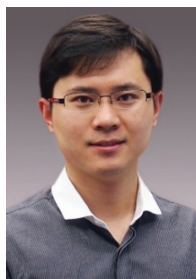
Civil and Environmental Engineering
Department, Rice University, 6100 Main St.
Houston, TX 77005, USA

Nancy P. Sanchez is a postdoctoral research associate at the Department of Civil and Environmental Engineering at Rice University. She received her BS degree in Chemical Engineering from the National University of Colombia, and a MS and PhD degree in Environmental Engineering from Los Andes University and the University of Akron. Her research interests include the monitoring and analysis of atmospheric contaminants in urban areas, and the application of spectrophotometric methods and multi-way data analysis for the study of environmental processes.

Wenzhe Jiang

Electrical and Computer Engineering
Department, Rice University, 6100 Main St.
Houston, TX 77005, USA

Wenzhe Jiang received his BSc degree in Microelectronics from Peking University in China in 2012. In August 2012, he joined the Laser Science Group at Rice University, Houston, TX, as a graduate student. His research at Rice is focused on the design and implementation of optical sensor platforms employing mid-infrared quantum cascade lasers and various spectroscopic techniques for trace gas detection. More specifically, his work at Rice is related to quartz enhanced photoacoustic spectroscopy and tunable laser absorption spectroscopy based optical sensor systems for environmental and biomedical applications.



Wei Ren

Mechanical and Automation Engineering
Department, Chinese University of Hong
Kong, New Territories, Hong Kong

Wei Ren is currently an Assistant Professor in the Department of Mechanical and Automation Engineering at the Chinese University of Hong Kong. He received his BS in Mechanical Engineering and MS in Optical Engineering from Tsinghua University in 2006 and 2008, respectively. He obtained his PhD degree in Mechanical Engineering from Stanford University in 2013. After his graduate work, Dr. Ren joined the Laser Science Group at Rice University as a postdoc research associate, where his research focused on trace gas sensing for environmental monitoring, industrial process control, and biomedical applications. Dr. Ren’s research to date has resulted in more than 20 peer-reviewed journal publications in the fields of combustion and propulsion, optical diagnostics and sensors, alternative fuels, and environmental research. Dr. Ren is a Member of the Optical Society (OSA), Society of Photo-Optical Instrumentation Engineers (SPIE), and Combustion Institute (CI).



Rafal Lewicki
Electrical and Computer Engineering
Department, Rice University, 6100 Main St.
Houston, TX 77005, USA

Rafal Lewicki received his MS and PhD degree (cum laude) in Electronics from Wroclaw University of Technology, Wroclaw, Poland in 2005 and 2011, respectively. Dr. Lewicki is currently a post doctoral fellow in the research group of Professor G. Wysocki at the Department of Electrical Engineering, Princeton University, Princeton, NJ. He held a post doctoral research associate position in the Department of Electrical and Computer Engineering at Rice University. His research interests are focused on trace gas detection using laser based spectroscopic techniques. He has specialized in the implementation of quantum cascade laser based optical sensor platforms, enabling high resolution, selective and real time spectroscopic measurements, for applications in environmental monitoring, medical diagnostics, and industrial process control.



Dongfang Jiang
Electrical and Computer Engineering
Department, Rice University, 6100 Main St.
Houston, TX 77005, USA

Dongfang Jiang received his BSc degree in Automation Engineering, MS and PhD degree in Control Theory and its Applications from NWPU in 1989, 1995, and 2000, respectively. He was a visiting scholar at the Electrical Engineering and Information Technology at Ruhr-Universitaet Bochum, Germany in 2002, and at the Laser Science Group at Rice University, USA in 2014. He is an associate Professor in the Department of Measurement and Control Technique and Instrumentations at Northwestern Polytechnical University (NWPU), China. Dr. Jiang is interested in real-time embedded systems, intelligent instruments, and automatic testing system designs. His current research focuses on optical measurement of air data, purification of noise corrupted weak signals, and the design of servo-systems primarily for aviation applications.



Robert J. Griffin
Civil and Environmental Engineering
Department, Rice University, 6100 Main St.
Houston, TX 77005, USA

Robert Griffin is Professor of Civil and Environmental Engineering. He received his BS from Tufts University in 1993, his MS 1997 and his PhD 2000 from Caltech. Dr. Griffin's research interests include performing field, laboratory, and computational experiments designed to understand the effects and behavior of organic species in the troposphere. He is a member of the American Association of Aerosol Research, the American Chemical Society, and the American Geophysical Union.



Frank K. Tittel
Electrical and Computer Engineering
Department, Rice University, 6100 Main St.
Houston, TX 77005, USA
fkt@rice.edu

Frank K. Tittel is the Josephine S. Abercrombie Professor of Electrical Computer Engineering at Rice University, where he also holds a joint faculty appointment in the Department of Bioengineering. He obtained his bachelor, master, and doctorate degrees in physics from the University of Oxford in 1955 and 1959, respectively. From 1959 to 1967 he was a Research Physicist with General Electric Research and Development Center, Schenectady, New York. Since 1967 he has been on the faculty at Rice University in Houston, TX. Dr. Tittel is a Fellow of the IEEE, the Optical Society of America and the American Physical Society. Current research interests include various aspects of quantum electronics, specifically laser spectroscopy and laser applications in environmental monitoring, industrial process control and medicine.